# Heavy Fermion Superconductivity in Non-magnetic Cage Compound $PrV_2Al_{20}$

**Yosuke Matsumoto, Masaki Tsujimoto, Takahiro Tomita, Akito Sakai and Satoru Nakatsuji**

Institute for Solid State Physics, University of Tokyo, Kashiwa 277-8581, Japan

E-mail: matsumoto@issp.u-tokyo.ac.jp

**Abstract.** $PrT_2Al_{20}$ ($T$ = Ti, V) are ideal systems to study the quadrupole Kondo effect and quantum criticality arising from orbital degrees of freedom. Both systems have the nonmagnetic cubic $\Gamma_3$ crystal electric field ground doublet with the well separated excited state. In particular, $PrV_2Al_{20}$ exhibits anomalous metallic behavior above and below the multipolar ordering temperatures, reflecting the even stronger hybridization between $f$ and conduction electrons possibly due to a proximity to a orbital quantum critical point. Here, we discuss the heavy fermion superconductivity (SC) of $PrV_2Al_{20}$ in detail. The SC appears at $T_c = 0.05$ K with the highly enhanced effective mass ($m^*/m_0 \sim 140$) estimated using the temperature dependence of the upper critical field. In addition, large electronic specific heat coefficient of $\gamma \sim 0.9$ J/mol K$^2$ above $T_c$ and the large specific heat jump at $T_c$ of $\Delta C/T_c \sim 0.3$ J/mol K$^2$ provide direct evidences of the heavy fermion SC. This observation indicates the first realization of the novel SC arising from the orbital fluctuation of the $f$ electrons at ambient pressure.

## 1. Introduction

In the $f$ electron intermetallics, a lot of interesting quantum states, such as exotic superconductivity (SC) with highly enhanced effective mass and non-Fermi liquid, have been reported in the vicinity of magnetic quantum critical points (QCPs) and have been extensively studied for the past few decades[1, 2, 3]. In this case, a competition between Kondo effect and RKKY interaction results in a quantum phase transition between Fermi liquid and a magnetically ordered state of $f$ electrons. On the other hand, it is an interesting open question what happens in the case of orbital QCPs which emerges on the border of $f$ electrons' orbital ordered states. This is highly non-trivial problem because hybridization effect between $f$ electrons' orbital degrees of freedom and conduction electrons is already exotic. The hybridization effect has been studied in the impurity model known as 2-channel (or quadrupolar) Kondo model in the nonmagnetic cubic $\Gamma_3$ crystal electric field (CEF) doublet of $f^2$ state[4], where non-Fermi liquid ground state and residual entropy were suggested. However, it is not established both theoretically and experimentally what happens in the lattice systems. Therefore, it is even more non-trivial problem what happens at the orbital QCP where the strong hybridization suppresses the orbital ordering.

In order to study this highly non-trivial problem, it is important to choose a material which has purely orbital degrees of freedom in the ground state. Such examples can be found in cubic non-magnetic $\Gamma_3$ doublet systems of a $f^2$ configuration. Intensive studies have revealed various interesting phenomena in the cubic $\Gamma_3$ doublet systems, in particular, in Pr-based intermetallic

Content from this work may be used under the terms of the Creative Commons Attribution 3.0 licence. Any further distribution of this work must maintain attribution to the author(s) and the title of the work, journal citation and DOI.
Published under licence by IOP Publishing Ltd

compounds[5, 6, 7, 8, 9]. However, Pr-based cubic $\Gamma_3$ doublet systems usually have well-localized $f$ moments, and thus there has been no prototypical system where we can study the orbital instability by tuning the hybridization between $f$ and conduction electrons.

On the other hand, recent studies have revealed that $PrT_2Al_{20}$ ($T$ = Ti, V) are ideal systems to study the quadrupole Kondo effect and quantum criticality arising from orbital degrees of freedom, where we can tune the $c$-$f$ hybridization by chemical substitution and by pressure[10, 11]. The both systems have the nonmagnetic cubic $\Gamma_3$ CEF doublet with the well separated excited state at $\Delta_{\rm CEF}$ ∼60 K (Ti) and 40 K (V)[10, 12, 13]. In addition, strong hybridization is expected in these compounds, from a caged structure with 16 Al ions surrounding $T$ ions. Indeed, the hybridization is strong as is evident in many physical properties[10, 14, 15, 16]. In particular, $PrV_2Al_{20}$ exhibits anomalous metallic behavior above and below the multipolar ordering temperatures, reflecting the even stronger hybridization due to a smaller size of the cage.

While a ferro-quadrupole (FQ) ordering (at $T = 2.0$ K) was observed in $PrTi_2Al_{20}$[10, 12, 17], double multipolar orderings at temperatures $T = 0.65$ and 0.75 K were observed in $PrV_2Al_{20}$[16, 18]. The observation of the multipolar orderings ensures that the degeneracy of $\Gamma_3$ doublet remains at least down to the ordering temperature. Note that these are non-Kramers systems and the degeneracy can be easily removed by disorders in the crystals.

Interestingly, both of these compounds exhibit heavy fermion SC inside the mutipole ordering phases[11, 16, 19]. In $PrTi_2Al_{20}$, the SC is highly enhanced under pressure of 8 GPa, where FQ ordering starts to be suppressed. The transition temperature ($T_c$) at ambient pressure (∼0.2 K) increases up to ∼ 1 K and the effective mass reaches $m^*/m_0 \sim 110$[11]. This strongly suggests a novel heavy fermion SC emerges in the vicinity of the orbital QCP. In this paper, we discuss the experimental observations made in the resistivity and specific heat measurements, which suggest strong orbital fluctuation in $PrV_2Al_{20}$. We also discuss the correspondence between the resistivity measurements and the specific heat measurements, where we observed the double transition. Then we discuss the heavy fermion SC of $PrV_2Al_{20}$ in detail. The SC appears at $T_c = 0.05$ K with the highly enhanced effective mass ($m^*/m_0 \sim 140$) even at ambient pressure[16]. In addition, large electronic specific heat coefficient of $\gamma \sim 0.9$ J/mol K$^2$ above $T_c$ and the large specific heat jump at $T_c$ of $\Delta C/T_c \sim 0.3$ J/mol K$^2$ provide direct evidences of the heavy fermion SC. This observation indicates the first realization of the novel SC arising from the orbital fluctuation of the $f$ electrons at ambient pressure. Note that a part of the results presented in this paper has been already discussed in the previous works[10, 16, 20, 21].

## 2. Experimental

Single crystals of $RT_2Al_{20}$ ($R$ = Pr, La, $T$ = Ti, V) were grown by the Al self-flux method[10]. We have succeeded in growing high quality single crystals, whose residual resistivity ratio (RRR) reaches ∼ 20, by tuning the starting ratio. Single and powder X-ray diffraction and SEM-EDX measurements indicate high quality and single phase of obtained crystals. The electrical resistivity $\rho(T)$ was measured by a low-frequency ac four-terminal method below ∼ 1 K using $^3$He-$^4$He dilution refrigerator. A dc four-terminal method was used above $T = 0.3$ K in conjunction with a commercial system (PPMS, Quantum Design). In this paper, residual resistivity ratio (RRR) is roughly defined as the ratio between the values at 300 K and lowest temperature above $T_c$ of the SC transition. The specific heat was measured using a relaxation method using a specific heat cell installed in a $^3$He-$^4$He dilution refrigerator. The ac- and dc-susceptibility measurements were performed by using a home-made magnetometer comprising a commercial SQUID sensor (Tristan Technologies) installed in a dilution refrigerator. For these specific heat and ac- and dc-susceptibility measurements, a pure single crystal with RRR ∼ 20 (0.111 mg) was used. The details were already discussed in the previous work[16].

## 3. Results and Discussions

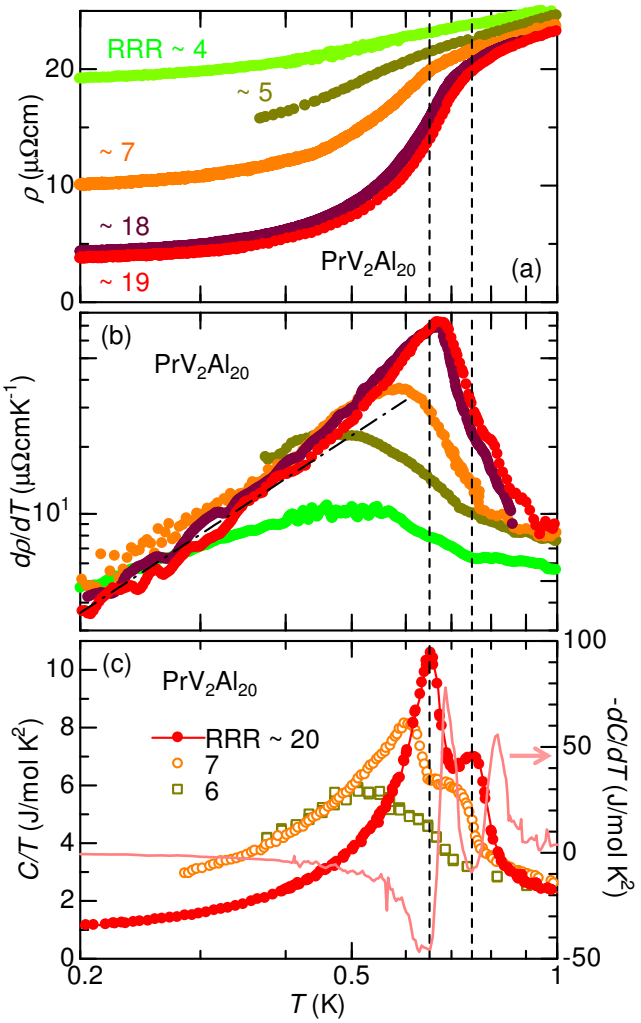



**Figure 1.** (a) Temperature dependence of the resistivity $\rho$ for various single crystals of $PrV_2Al_{20}$ with different sample qualities. (b) Full logarithmic plot of $d\rho/dT$ versus temperature for the data presented in (a). The dashed-dotted line indicates a power law temperature dependence of $d\rho/dT \propto T^2$. (c) Specific heat $C$ divided by temperature $T$, $C/T$, for the samples with different RRRs (left axis) and $-dC/dT$ for the sample with RRR = 19 (right axis). Here, the lattice contribution is already subtracted by using $C/T$ for $LaV_2Al_{20}$. The results for the sample with RRR = 6, 7 are from the previous works[10, 18]. The vertical broken lines in (a), (b), (c) indicate the transition temperatures $T_Q$ = 0.75 K and $T^*$ = 0.65 K for RRR = 20 defined as the peak temperatures in $C/T$ in the previous works[16, 20].

First we present the temperature dependence of the resistivity $\rho$ for various single crystals of $PrV_2Al_{20}$ around multipolar ordering temperatures in Figure 1 (a). Depending on the sample quality, the resistivity drops below the ordering temperatures are different to each other. Correspondingly, the temperature derivative of the resistivity, $d\rho/dT$, indicates a systematic change depending on the sample quality as shown in Figure 1 (b). The samples with higher RRR indicate a sharper peak in $d\rho/dT$ at the multipolar ordering temperatures. Interestingly, $d\rho/dT$ for different quality samples overlap on top in the temperature range well below the multipolar ordering temperatures, especially for the sample with RRR $\sim$ 19, 18, 7. The observed temperature dependence is consistent with a power law behavior $d\rho/dT \propto T^2$ which is indicated by the dashed line in the figure and is consistent with the power law behavior $\Delta\rho \propto T^3$ reported in the previous work[21]. Here, $\Delta\rho$ is defined as $\Delta\rho \equiv \rho - \rho_0$, where $\rho_0$ is the residual resistivity estimated above $T_c$. The power law behavior suggests the strong orbital fluctuation even below the orbital ordering temperatures.

We also present the specific heat $C$ divided by temperature $T$, $C/T$, for the samples with different RRRs in Figure 1 (c), in order to see the correspondence to the resistivity data. Here, the lattice contribution is already subtracted by using $C/T$ for $LaV_2Al_{20}$. As already discussed in the previous works[16, 20], a broad single peak observed for RRR $\sim$ 6 separates into a sharp double peak structure for RRR $\sim$ 7 and 20. The peak structure which becomes sharper as RRR

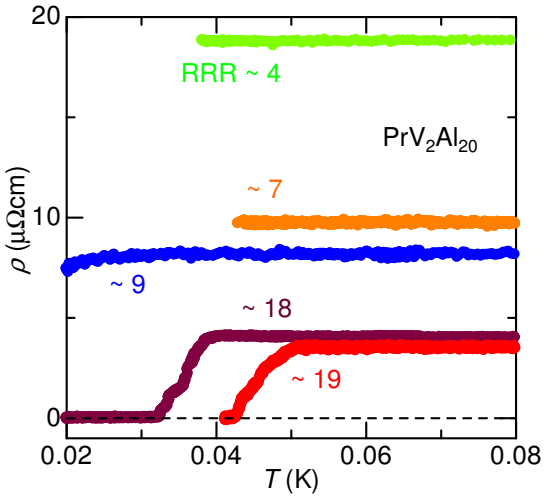



**Figure 2.** Temperature dependence of the resistivity $\rho$ for various single crystals of $PrV_2Al_{20}$ with different sample qualities at the lowest temperatures below $T \sim 0.08$ K.

increases strongly indicates that the double transition is intrinsic behavior in this compound. In the previous works[16, 20], the transition temperatures $T_Q = 0.75$ K and $T^* = 0.65$ K for RRR = 19 were defined by the peak temperatures in $C/T$ as indicated by the vertical broken lines in the Figures 1 (a), (b), (c). Note that these temperatures are designated following the previous work[18] and we do not intend to refer to any specific order parameter in this paper. As seen in Figures 1 (a) and (b), there is no clear indication of the double transition in the resistivity data even for the samples with almost the same quality. If we dare to see the correspondence between $\rho$ for the sample with RRR = 19 and $C$ for the sample with RRR = 20, $T^* = 0.65$ may correspond to the peak in $d\rho/dT$ and $T_Q = 0.75$ may correspond to the temperature where $d\rho/dT$ becomes most steep (Fig. 1 (b)). We also present $-dC/dT$ for the sample with RRR = 20, which is indicated by the solid line in Figure 1 (c). Alternatively, it is also possible to associate the peak in $-dC/dT$ found at $T \sim 0.69$ K with the peak in $d\rho/dT$. Another peak in $-dC/dT$ found at $T \sim 0.82$ K, then, may correspond to the temperature where $d\rho/dT$ starts to rise on cooling. In order to see further correspondence or to obtain further insight on the order parameters of the multipolar orderings, more studies including those using macroscopic/microscopic probes are indispensable.

Next we discuss the SC found inside the multipolar ordered state of $PrV_2Al_{20}$ under the strong orbital fluctuations. As clearly seen in Figure 2, the sample with RRR $\sim$ 19 exhibits a resistivity drop due to the SC transition at $T_c = 0.05$ K. The SC transition was also found in another sample (RRR $\sim$ 18) at a slightly lower $T_c = 0.039$ K. The sample with RRR $\sim$ 9 exhibit a slight drop of the resistivity at $T \sim 0.02$ K. This is supposed to be the SC because it exhibits further drop reaching $\sim 4$ $\mu\Omega$cm in the lower temperatures where the thermometer is not calibrated and is suppressed under a weak field of the order of 10 mT applied along [110] direction (not shown). On the other hand, we did not find any sign of SC at least down to 38 and 43 mK for the sample with RRR $\sim$ 4 and 7, respectively. The results suggest that $T_c$ strongly depends on RRR, which may indicate an unconventional character of the SC. Apparently, further measurements are required to confirm the RRR dependence.

The bulk superconductivity was confirmed by dc- and ac-susceptibility measurements of a high quality crystal (RRR $\sim$ 20). Figure 3 (a) shows the $T$ dependence of the dc-susceptibility $\chi(T)$ of $PrV_2Al_{20}$ under a field of $\mu_0 H = 0.1$ mT along the [110] direction. The unit of $\chi(T)$ is calibrated by using the perfect diamagnetic signal of the reference Al sample with the same dimension placed in the canceling coil. The volume fraction was estimated to be 82% (ZFC) and 47% (FC), indicating the bulk SC. Note that the susceptibility for the perfect diamagnetism of the sample is estimated to be $-1.15$ emu/cc, considering the diamagnetic correction factor

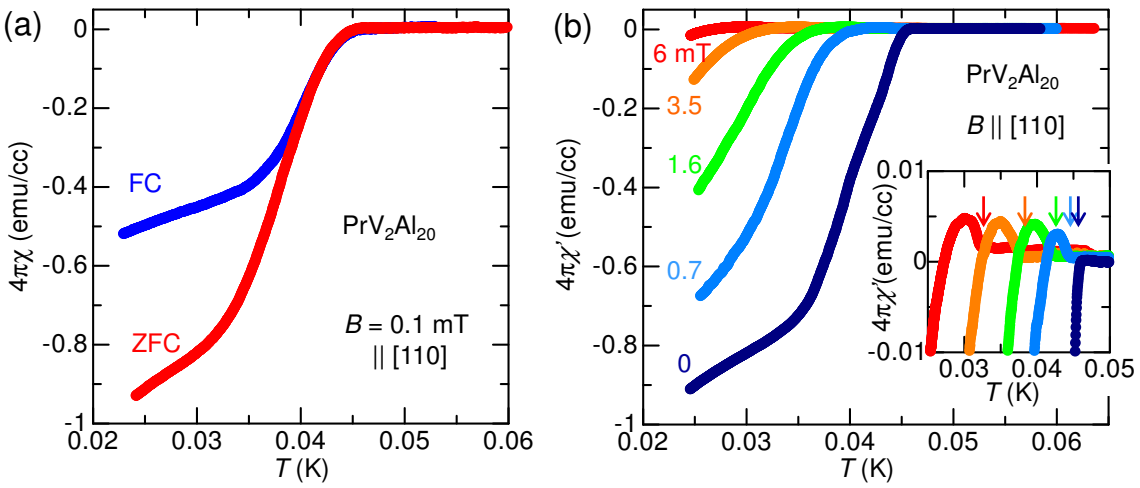



**Figure 3.** (a) Temperature dependence of the dc-susceptibility $\chi(T)$ for the single crystal of $PrV_2Al_{20}$ (RRR $\sim$ 20) under the field of 0.1 mT for zero field cooled (ZFC) and field cooled (FC) sequences. (b) Real part of the ac-susceptibility $\chi'(T)$ for the same $PrV_2Al_{20}$ sample. Inset shows an enlarged view around $T_c$. The arrows indicate $T_c$ defined as the onset of the anomaly.

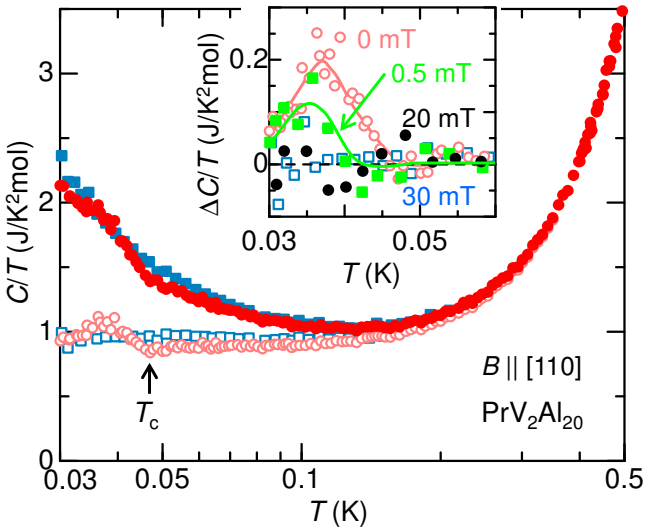



**Figure 4.** Temperature dependence of $C/T$ (closed circles). Here, the lattice contribution is subtracted by using $C/T$ for $LaV_2Al_{20}$. $C_{4f}/T$ obtained after subtracting the nuclear contribution $C_n/T$ is also shown (open circles). Inset shows $\Delta C/T$ obtained after subtracting $\gamma$ from $C_{4f}/T$ at the lowest temperatures around $T_c$. In addition to the zero-field data, those in the weak magnetic field along the [110] direction are also shown. See text for details.

$D \sim 0.13$. The large diamagnetic signal comparable to the Al shielding signal is also observed in the $T$ dependence of the real part of the ac-susceptibility $\chi'(T)$ under zero dc-field and ac-field $\sim 0.1$ $\mu$T as shown in Figure 3 (b). Here, $T_c$ was determined by the onset of the anomaly of the ac-susceptibility as shown by the arrows in Figure 3 (b) inset. Compared to $PrTi_2Al_{20}$, the peak in the susceptibility around $T_c$ due to differential paramagnetic effect is quite small in $PrV_2Al_{20}$[22], indicating strong pinning effect typical to the type II SC.

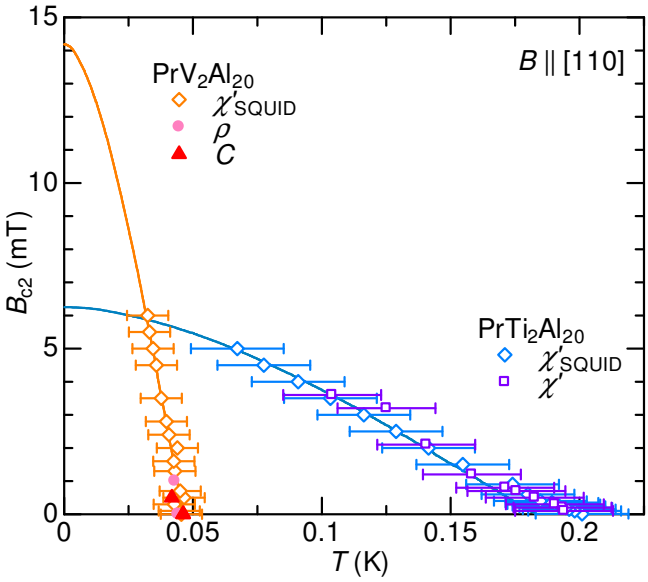



**Figure 5.** $T$ dependence of the upper critical field $B_{c2}$ for the single crystals of $PrV_2Al_{20}$ (RRR $\sim$ 20) and $PrTi_2Al_{20}$ (RRR $\sim$ 150) under a field along [110]. The square/diamond/circle/triangle data points are determined by ac-susceptibility with a standard technique, ac-susceptibility by SQUID, resistivity, and specific heat measurements, respectively. Solid lines represent the fit based on the WHH model.

Furthermore, the bulk heavy fermion SC is confirmed by the specific heat data. We present $C/T$ below 0.5 K in Figure. 4. In the lower temperatures, the data exhibit a slight increase on cooling below 0.12 K and finally indicate an anomaly due to SC transition at $T = 0.046$ K. The low $T$ upturn in $C/T$ becomes evident in the normal state stabilized under the magnetic field of 30 mT and is found to follow $C/T \sim T^2$ down to the lowest $T$ of 30 mK. As already discussed in the previous work[16], this contribution is most likely arising from a hyperfine enhanced nuclear magnetism. The $4f$-electron contribution of the specific heat divided by $T$, $C_{4f}/T$ is obtained after subtracting $C_n/T \sim T^{-2}$ coming from the nuclear magnetism. The zero-field SC anomaly is clearly seen in $C_{4f}/T$, which is shown in the figure by the open circles. This confirms the bulk character of the SC. The nearly constant $C_{4f}/T$ in the normal state provides an estimate of the large electronic coefficient $\gamma \sim 0.9$ J/molK$^2$. The SC jump in $C/T$ is evaluated using the temperature dependence of $\Delta C/T \equiv C_{4f}/T - \gamma$, as is shown in the inset of Figure 4. The jump reaches 0.3 J/molK$^2$, which provides direct evidence of the heavy-fermion SC. The ratio obtained from the jump, $\Delta C/\gamma T_c \sim 0.3$ is much smaller than the BCS value of 1.43. As already discussed in the previous work[16], the above estimated jump can be further increased if the sample quality is improved, which is the one of the important future issues. In the inset of Figure 4, $\Delta C/T$ in weak magnetic fields are also shown. The SC anomaly is slightly suppressed at $B = 0.5$ mT with $T_c = 0.042$ K and is not observed at $B = 20$ and 30 mT.

Figure 5 shows the $T$ dependence of the upper critical field $B_{c2}$ estimated using the ac-susceptibility, resistivity and specific heat data for $PrV_2Al_{20}$. For comparison, we show the results for $PrTi_2Al_{20}$ as well [19]. The solid line in Fig. 5 is the fit to our $B_{c2}$ results based on the Werthamer-Helfand-Hohenberg (WHH) model [23, 24]. The best fitting was obtained using parameters of $T_c = 46.2$ mK and the slope of $B_{c2}$ at $T_c$, $B'_{c2} \equiv dB_{c2}/dT = 0.41$ T/K. The model reproduces the experimental data well, indicating the orbital depairing effect is dominant. The resultant orbital critical field at $T = 0$, $B_{c2}^{orb}(0) = -0.727 B'_{c2} T_c$, and Ginzburg-Landau (GL)

coherence length, $\xi = \sqrt{\Phi_0/2\pi B_{c2}^{orb}(0)}$, are $B_{c2}^{orb}(0) = 14.3$ mT and $\xi = 0.15$ $\mu$m, respectively.

Surprisingly, $B'_{c2}$ of $PrV_2Al_{20}$ is about 10 times larger than the Ti analog [19], indicating significantly heavier effective mass. Indeed, the effective mass is estimated to be $m^* = \hbar k_F/v_F \sim 140m_0$ by using the GL coherence length $\xi = 0.15$ $\mu$m, the Fermi velocity $v_F = \xi k_B T_c/(0.18\hbar) = 5.1$ km/s, $k_F = (3\pi^2 Z/\Omega) = 6.1 \times 10^9$ m$^{-1}$, where $Z$ is the number of electrons per unit cell, and $\Omega$ is the unit-cell volume. The effective mass $m^*/m_0 \sim 140$ is much larger than $m^*/m_0 \sim 16$ estimated for $PrTi_2Al_{20}$ under ambient pressure [19], is comparable to $m^*/m_0 \sim 110$ under $\sim 8$ GPa in the vicinity of the quadrupolar quantum criticality [11]. Thus, the mass enhancement in $PrV_2Al_{20}$ indicates not only the strong $c$-$f$ hybridization, but its proximity to a quadrupolar QCP.

## 4. Conclusion

In this paper, we discussed the experimental observations made in the resistivity and specific heat measurements, which suggest strong orbital fluctuation in $PrV_2Al_{20}$. We also discussed the correspondence between the resistivity measurements and the specific heat measurements, where we observed the double transition. Then we discussed the properties of the heavy fermion SC in $PrV_2Al_{20}$ in detail. The SC appears at $T_c = 0.05$ K for the sample with RRR = 19. The strong RRR dependence of $T_c$ may indicate an unconventional character of the SC. The bulk superconductivity was confirmed by dc- and ac-susceptibility measurements and specific heat measurements made for the same high quality single crystal with RRR $\sim$ 20. Large electronic specific heat coefficient of $\gamma \sim 0.9$ J/mol K$^2$ above $T_c$ and the large specific heat jump at $T_c$ of $\Delta C/T_c \sim 0.3$ J/mol K$^2$ provide direct evidences of the heavy fermion SC together with the highly enhanced effective mass ($m^*/m_0 \sim 140$) estimated using the temperature dependence of the upper critical field. This observation indicates the first realization of the novel SC arising from the orbital fluctuation of the $f$ electrons at ambient pressure. In order to establish the role of orbital fluctuation in the heavy fermion SC found in $PrV_2Al_{20}$, comprehensive studies including those using macroscopic/microscopic probes in conjunction with high pressure and magnetic fields are quite important. Further improvement of the sample quality is also the important future issue.


## Acknowledgments

We thank Y. Uwatoko, K. Matsubayashi, J. Suzuki, T. Sakakibara, Y. Shimura, K. Araki, Y.-B. Kim, K. Kuga, K. Hattori and K. Ueda for their support and the useful discussions. This Letter was partially supported by PRESTO of JST and Grants-in-Aid (Nos. 25707030 and 90422443) from the Japanese Society for the Promotion of Science (JSPS), by Grants-in-Aids for Scientific Research on Innovative Areas " Heavy Electrons "and Scientific Research on Innovative Areas (15H05882, 15H05883) of the Ministry of Education, Culture, Sports, Science and Technology, Japan. The use of the facilities of the Materials Design and Characterization Laboratory at the Institute for Solid State Physics, The University of Tokyo is gratefully acknowledged. One of the authors, (M. T.) was supported by the JSPS through Program for Leading Graduate Schools (MERIT).


## References


[1] Stewart G R 2001 *Rev. Mod. Phys.* **73** 797
[2] Löhneysen H v, Rosch A, Vojta M and Wölfle P 2007 *Rev. Mod. Phys.* **79** 1015
[3] Monthoux P, Pines D and Lonzarich G G 2007 *Nature* **450** 1177
[4] Cox D L 1987 *Phys. Rev. Lett.* **59** 1240
[5] Morin P, Schmitt D and du Tremolet de Lacheisserie E 1982 *J. Magn. Magn. Mater.* **30** 257
[6] Suzuki H, Kasaya M, Miyazaki T, Nemoto Y and Goto T 1997 *J. Phys. Soc. Jpn.* **66** 2566
[7] Onimaru T, Sakakibara T, Aso N, Yoshizawa H, Suzuki H S and Takeuchi T 2005 *Phys. Rev. Lett.* **94** 197201

[8] Onimaru T, Matsumoto K T, Inoue Y F, Umeo K, Saiga Y, Matsushita Y, Tamura R, Nishimoto K, Ishii I, Suzuki T and Takabatake T 2010 *J. Phys. Soc. Jpn.* **79** 033704
[9] Onimaru T, Matsumoto K T, Inoue Y F, Umeo K, Sakakibara T, Karaki Y, Kubota M and Takabatake T 2011 *Phys. Rev. Lett.* **106** 177001
[10] Sakai A and Nakatsuji S 2011 *J. Phys. Soc. Jpn.* **80** 063701
[11] Matsubayashi K, Tanaka T, Sakai A, Nakatsuji S, Kubo Y and Uwatoko Y 2012 *Phys. Rev. Lett.* **109** 187004
[12] Sato T J, Ibuka S, Nambu Y, Yamazaki T, Hong T, Sakai A and Nakatsuji S 2012 *Phys. Rev. B* **86** 184419
[13] Koseki M, Nakanishi Y, Deto K, Koseki G, Kashiwazaki R, Shichinomiya F, Nakamura M, Yoshizawa M, Sakai A and Nakatsuji S 2011 *J. Phys. Soc. Jpn.* **80** SA049
[14] Matsunami M, Taguchi M, Chainani A, Eguchi R, Oura M, Sakai A, Nakatsuji S and Shin S 2011 *Phys. Rev. B* **84** 193101
[15] Tokunaga Y, Sakai H, Kambe S, Sakai A, Nakatsuji S and Harima H 2013 *Phys. Rev. B* **88** 085124
[16] Tsujimoto M, Matsumoto Y, Tomita T, Sakai A and Nakatsuji S 2014 *Phys. Rev. Lett.* **113** 267001
[17] Ito T U, Higemoto W, Ninomiya K, Luetkens H, Baines C, Sakai A and Nakatsuji S 2011 *J. Phys. Soc. Jpn* **80** 113703
[18] Araki K, Shimura Y, Kase N, Sakakibara T, Sakai A and Nakatsuji S 2014 *JPS Conf. Proc.* **3** 011093
[19] Sakai A, Kuga K and Nakatsuji S 2012 *J. Phys. Soc. Jpn* **81** 083702
[20] Tsujimoto M, Matsumoto Y and Nakatsuji S 2015 *J. Phys. Conf.: Ser.* **592** 01023
[21] Matsumoto Y, Tsujimoto M, Tomita T, Sakai A and Nakatsuji S *to appear in J. Magn. Magn. Mater.*
[22] Hein R A and Falge R L 1961 *Phys. Rev.* **123** 407
[23] Werthamer N R, Helfand E and Hohenberg P C 1966 *Phys. Rev.* **147** 295
[24] Helfand E and Werthamer N R 1966 *Phys. Rev.* **147** 288